

# LRFD AND EUROCODE-3 SPECIFICATIONS FOR ULTIMATE LOAD CARRYING CAPACITY EVALUATION OF STEEL COLUMNS AND EFFECTS OF IMPERFECTIONS

Talha Ekmekyapar\*, Mustafa Özakça

**Abstract:** In this study main attention is focused on axial load carrying capacity of steel columns. Towards this aim, employing nonlinear geometric and material properties Finite Element models are generated using ANSYS program. In simulations due to its advantages Arc-Length method is utilized for determination of axial load capacity of columns. Computational study consists of four phases. In the first one nonlinear buckling loads of IPE 200 section are evaluated for different slenderness ratios ( $L/r_y$ ). Obtained results for different slenderness ratios are assessed against LRFD and Eurocode-3 specifications. In the second section geometrical imperfections are incorporated into column models in a systematic manner and capacity changes are evaluated. Effects of eccentric compression loadings on the axial load carrying capacity are studied in third section. Fourth section introduces the effects of combined geometrical imperfections and eccentric loadings.

**Keywords:** Steel column, Buckling, Nonlinear behaviour, LRFD and Eurocode-3, Imperfections

## 1. Introduction

In most cases the real field structural elements have many differences than designed structure owing to some reasons, such as construction errors and fabrication defects. These defects and errors bring about some geometrical imperfections that cause reduction in ultimate strength of structural elements. The presence of geometrical imperfections leads to significant reduction of the capacity of such members. As a result, the real ultimate load carrying capacity cannot reach the limit which was obtained from perfect structure. Although this case is commonly known, no certain guidelines exist for the modeling of imperfections. The design codes and standards generally provide only conservative limits for the magnitude of imperfections and defects to be used in design of structural elements.

Also the belief of the ideal column as a purely compression member is usually not valid, due to eccentricities which exist in practice, especially in the border and corner of structures. If a compressive force acts eccentrically, the element is subjected to additional bending forces and this leads to reduction of ultimate capacity. So, the ability to precisely predict the ultimate capacity and post-buckling behavior of columns considering geometrical imperfections and eccentric loading is therefore essential for structural engineering. Many studies concerning these effects have been presented in the literature over the decades. One heading that is not documented in any detail is the post-buckling response of columns subjected to eccentric loadings with geometrical imperfections.

Satisfying results have been obtained in the past for prediction of nonlinear behavior of steel structures via a numerical technique of finite elements (FE). Behavior of stainless steel plates in compression were investigated in the past (Rasmussen et al., 2003). Authors presented FE models for steel plates and showed that excellent agreement with tests can be achieved. Bending and axial compression interaction of steel members with the main focus of

---

\* Department of Civil engineering, University of Gaziantep, Gaziantep. E-posta: [ekmekyapar@gantep.edu.tr](mailto:ekmekyapar@gantep.edu.tr)

developing design formulae accounting for stress strain nonlinearity, initial geometric imperfections and residual stresses was studied (Greiner and Kettler, 2008). In further studies mechanical behaviors of high strength steel thin-walled box section stub columns loaded in compression in order to suggest a modified design principle (Gao et al.2009). The stability of large diameter thin-walled tube beam columns was investigated taking initial imperfection, slenderness ratio and the bending moment ratio as parameters (Pan et al., 2008), while an imperfection sensitivity study of cold formed tubular steel columns at uniform elevated temperatures was conducted by (Feng et al., 2004).

I-shaped steel members represent the basic structural element in majority of steel structures. The wider use of these members in many areas of application has promoted considerable interest in the ultimate capacity of these members under compressive loads. Thus, it is important to accurately predict the post buckling behavior of such members for efficient structural designs. The interaction curves for locally buckled I-section beam-columns were investigated (Hasham and Rasmussen, 2002). To study the effect of the interaction between flange and web width-thickness ratio along with member slenderness ratio on behavior of columns fabricated from slender I-sections FE models were used (Salem et al., 2004). Elastic stability of eccentrically loaded steel columns with tapered and stepped I-sections and initial imperfections was investigated (Raftoyiannis and Ermopoulos, 2005). On the other hand numerical and experimental studies were conducted on the local-overall interaction buckling behavior and ultimate capacity load of I-section steel columns (Ren and Zeng, 1997).

Employing the FE method and incorporating non-linear material and geometric analysis procedures, it is possible to model the post-buckling behavior of columns. The present paper is devoted to investigation of effects of geometrical imperfections and loading eccentricities on the stability and post-buckling behavior of IPE 200 column with different slenderness ( $L/r_y$ ) ratios. In this study the global modes of failure was investigated. In post-buckling studies generally the lowest buckling modes are frequently assumed to provide the most critical imperfections. Since the IPE 200 cross section is compact, no local mode of failure has to be expected. As a result, it is meaningful to study the global imperfections on the IPE 200 steel cross section. Instead of considering a constant column length, this paper considers a range of column lengths to evaluate these effects with global modes of failure.

## **2. Finite Element Model**

### **2.1 Model description**

Using ANSYS FE package a nonlinear FE model was established to evaluate the ultimate capacity of steel compression members. The used element is SHELL181 which is suitable for analyzing thin to moderately-thick shell structures. It is a 4-node element with six degrees of freedom at each node: translations in the x, y, and z directions, and rotations about the x, y, and z-axes. SHELL181 is well-suited for large rotation and can be associated with elasto-plastic material properties (ANSYS, 2007). The studied cross section is shown in Figure 1.

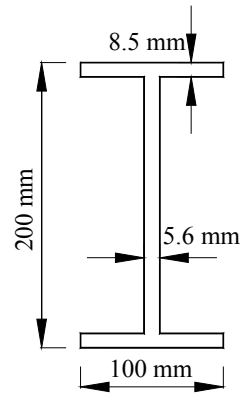


**Figure 1.** Cross section dimensions

The material was assumed to have elastic-perfectly plastic stress-strain relationship as shown in Figure 2, with values of Young's modulus ( $E$ ) and Poisson's ratio ( $\nu$ ) of 210 GPa and 0.3, respectively. The yield stress was  $\sigma_y=235$  MPa. The NLGEOM option of ANSYS was implemented to incorporate geometric nonlinearities into FE models. The arc-length path following method was employed to predict nonlinear response.

Study presented on the stability behavior of I Sections (Salem et al., 2004) considering the residual stresses in thin-walled prismatic columns having overall imperfection of  $L/1000$  showed that the maximum reduction in ultimate axial load is small enough to be neglected. The effect of residual stresses in the FE model on the ultimate capacity of columns is not taken into consideration in this study for simplicity.

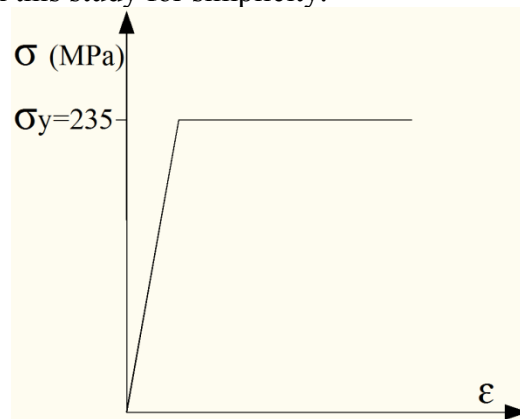


**Figure 2.** Elastic perfectly plastic material model

Owing to symmetry half of the columns were modeled. To satisfy simple support conditions translation in  $x$  and  $y$  directions and rotation around the  $z$  axis at the member end ( $z = 0$ ), and to satisfy the boundary conditions at the middle section ( $z = L/2$ ), is such that the translation in the  $z$  direction, rotations around the  $x$  and  $y$  axes are constrained as shown in Figure 3.

## 2.2 Geometric imperfections

Initial imperfection in structural members is a crucial factor that leads to uncertainty in the predictions of ultimate capacity. To investigate the effects of distortions for each different  $L/r_y$  ratios, the half sine wave bow imperfections were incorporated into the model with magnitudes of  $L/5000$ ,  $L/1000$  and  $L/500$  in a post-buckling analysis, from which load-deflection curves were obtained. The used sinusoidal imperfections are considered about minor axis and represented by as;

$$w_0 = \delta L \sin\left(\frac{\pi z}{L}\right) \quad (1)$$

where  $\delta$  is the maximum amplitude of overall imperfection,  $L$  is the column length and  $z$  is the  $z$  coordinate of corresponded node. The axial load is directly distributed to the nodes on the section at the member end ( $z = 0$ ) as shown in Figure 3.

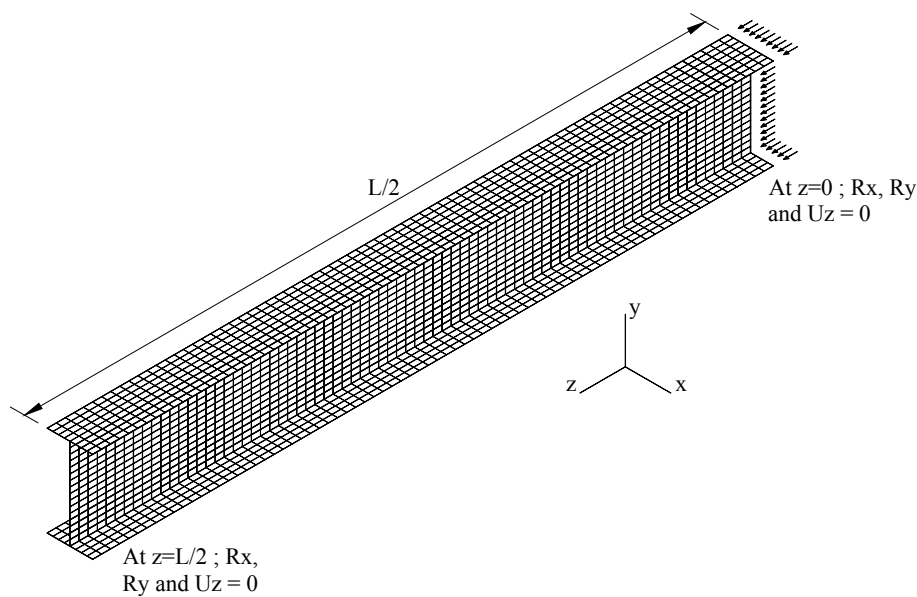


**Figure 3.** Finite element model of column for comparison purpose

## 2.3 Loading eccentricity

The eccentric loading was achieved by placing a rigid plate at the member end ( $z = 0$ ), of the cross section of the column as shown in Figure 4. The placed end plate affects the ultimate capacity of columns. Therefore, in order to integrate the imperfection and eccentricity models and clearly discuss the results, in the forthcoming analyses we shall consider this effect and create the FE models of entire study with end plate. In the case of only overall imperfection models the loading does not change and distributed on the section (boundary conditions applied nodes in Figure 5). Figure 4 illustrates the FE model of study.

In eccentric loading runs the load is applied as a point load to relevant nodes that is clearly defined in Figure 5. The placed end plate has big thickness and elastic modulus sufficient to distribute the stresses uniformly on the whole section. The boundary conditions defined in section 2.1 were applied only to the corresponded nodes of column cross section at the member end ( $z = 0$ ), as shown in Figure 5. The other nodes of rigid plate are free. Also the Figure 5 illustrates the nodes of eccentric loadings.

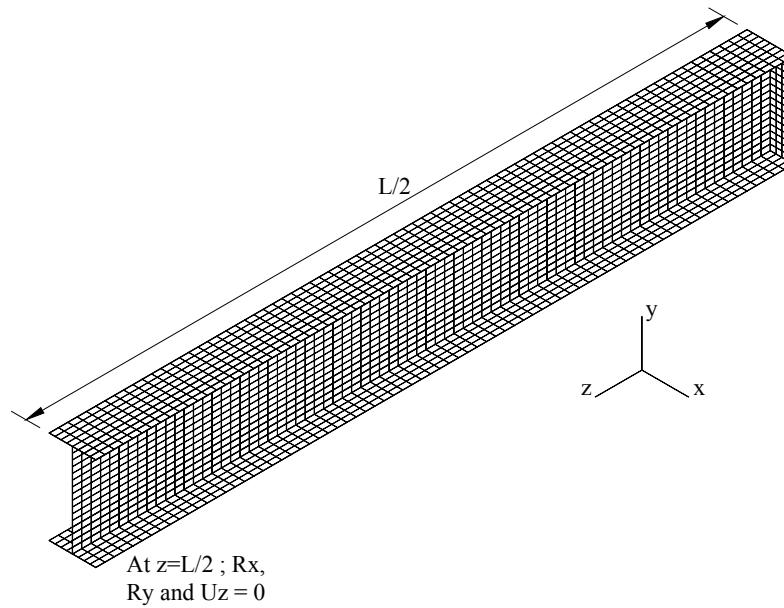


**Figure 4.** Finite element model of study

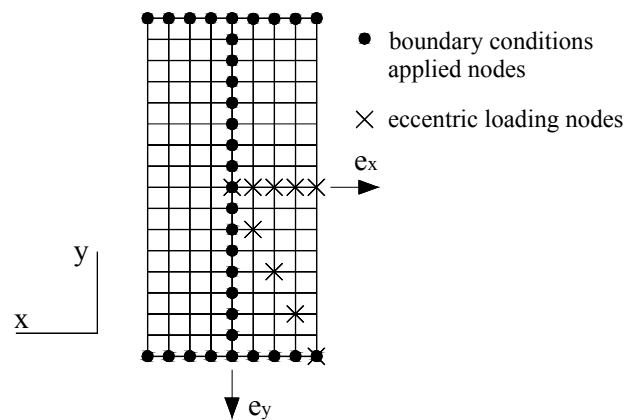


**Figure 5.** Rigid end plate details (At  $z=0$ )

It was intended to study collapse modes about minor axis of columns. So, eccentric loadings were based on mainly  $e_x$  direction as shown in Figure 5. Furthermore, in order to observe the  $e_y$  eccentricity effects along with  $e_x$  loadings, four additional points were established. But no effort has been exerted to generate collapse modes only about major axis. Therefore,  $e_y$  loadings without  $e_x$  eccentricity were not performed.

### 3. Numerical Simulations Against Specifications and Laboratory Tests

Before conducting the numerical studies, in order to assess the validity of models, comparison of results of generated FE model with some design specifications and pre-published experimental data was performed.

#### 3.1 Comparison with Eurocode-3 and AISC-LRFD specifications

The ultimate loads obtained by means of nonlinear FE analyses were compared by the design specifications (Eurocode-3., 2005; AISC-LRFD, 2005). The overall imperfections magnitudes of  $L/5000$ ,  $L/1000$  and  $L/500$  are incorporated into the IPE 200 models to capture nonlinear

stability behaviors. The end plate effects are not considered in design specifications. So in this section the FE model depicted in Figure 3 was used to make comparisons with design specifications. The results of FE analyses are presented in Table 1. The comparisons of FE results and design specifications are depicted in Figure 6 on the load vs. end shortening graphs.

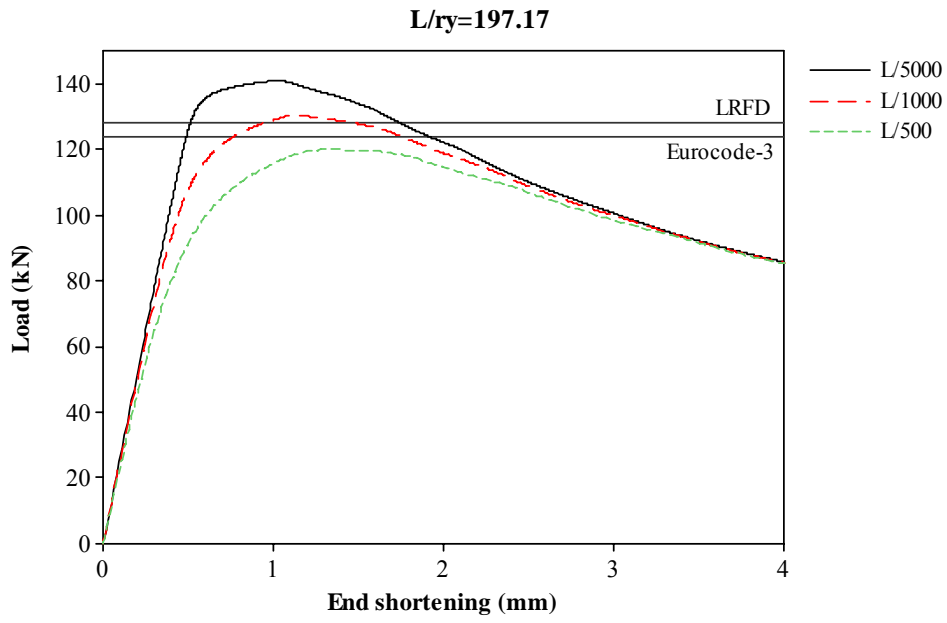
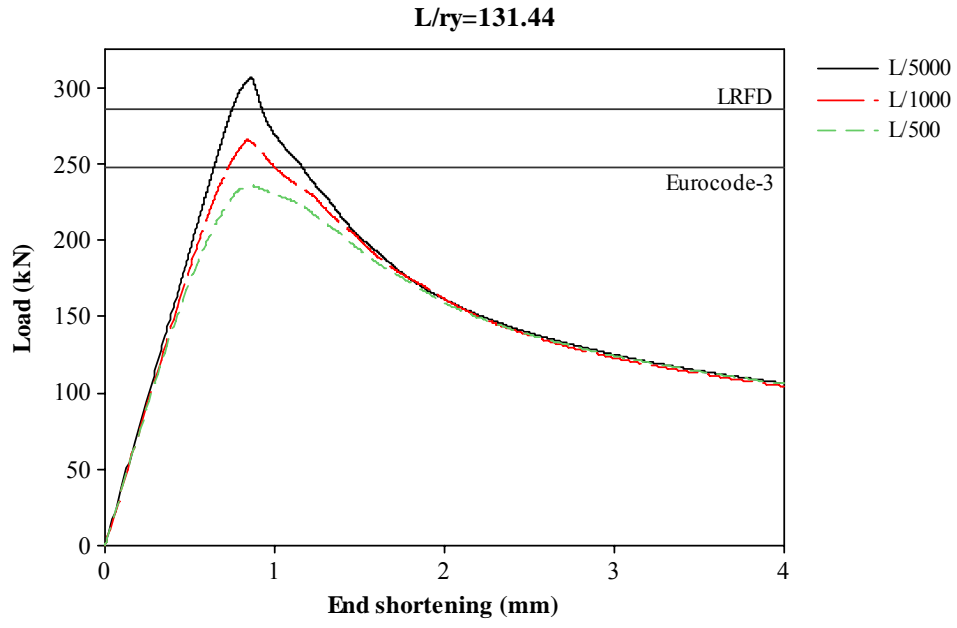
**Table 1.** Ultimate load values

Column Length	Slenderness ratio( $L/r_y$ )	Ultimate Load (kN)		
		Imperfection ( $\delta$ )		
		L/5000	L/1000	L/500
3.0 m	131.44	306.74	265.85	235.47
4.5 m	197.17	141.04	130.37	119.89
6.0 m	262.89	81.26	76.93	72.37

The results of post-buckling analyses in Table 1 and Figure 6 clearly demonstrate the degree of sensitivity to overall imperfections.

For 3m column length, with overall imperfection magnitudes of L/1000 and L/500 leading to reductions in failure load of approximately 13.3% and 23.2% respectively from that of the model with L/5000 overall imperfection. These reductions are approximately 7.6% and 15.0% with overall imperfections magnitudes of L/1000 and L/500 respectively for 4.5m column length, finally 5.3% and 10.9% for 6m column length. In light of the results presented above, it is clear that the percent effect of overall imperfection magnitude on ultimate load reduces with increase of the column length.

In this section the developed simulation model was assessed against Eurocode-3 and LRFD design specifications for the axially loaded steel columns. The obtained results exhibited good agreement with the design specifications. A 15.3 % difference in ultimate load evaluation was observed between the design specifications for the column which has 3 m length. However, it should be noted that discrepancy of ultimate load results of specifications reduced by the increase of column slenderness as displayed in Figure 6. And it is worth noting that as the simulation models are not perfect, have global mode of geometrical imperfections and possess nonlinear material and geometrical characteristics, the specifications evaluations are safe enough to account for underlying mechanics of axially loaded columns. Here it depends on design engineer to make a decision on which specification to use. Nevertheless it should be noted that the Eurocode-3 specification implies more equations to solve to evaluate ultimate load carrying capacity of a column. However LRFD specification has the potential to capture the ultimate load with solving a few equations for the case in present study. The difference of two design specifications in the evaluation process originates from use of different buckling curves. The Eurocode-3 relies on four buckling curves (curves a, b, c, and d) in the evaluation process, while LRFD approach employs single curve through capacity evaluations of columns. But more studies, such as works on capacity evaluation of beam-columns and non-compact sections, need to be performed to make a general assessment of referred design specifications.



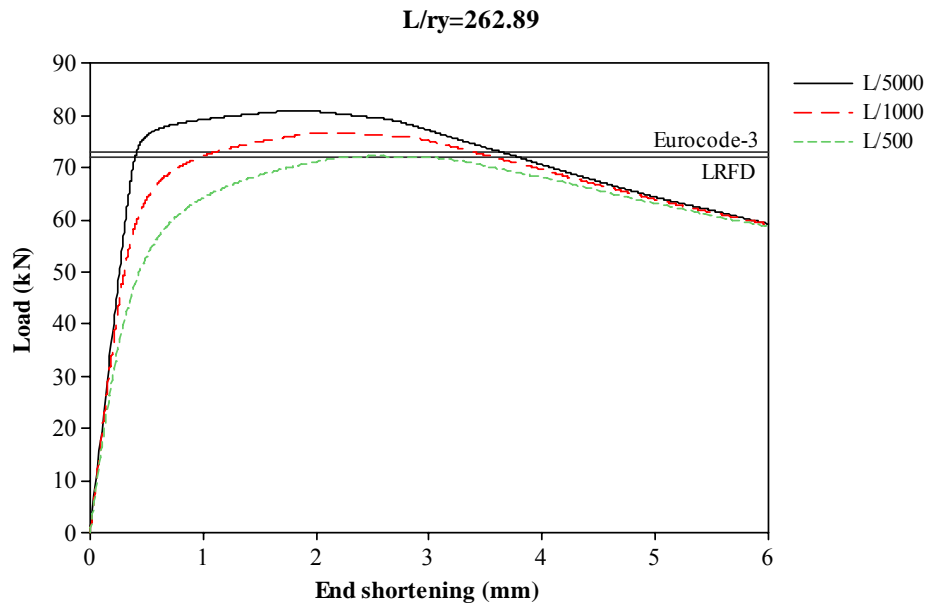


**Figure 6.** Load versus end shortening curves and results of design specifications

### 3.2 Comparison with experimental results

In order to verify the developed FE model, the experimental results presented on long I-section columns were used (Davids and Hancock, 1986). The study in literature focused on fabricated columns by welding three plates of same width and thickness (5mm), with values of Young' Modulus ( $E$ ) and yield stress ( $\sigma_y$ ) of 200 GPa and 350 MPa respectively. The overall geometric imperfections measured by Davids and Hancock [13] were less than  $L/5000$ . The developed simulation model in present study neglects the residual stresses and includes  $L/1000$  overall geometric imperfection. They named the specimens according to width of used plates and specimen length. Two specimens from their experimental set first has 310 mm and second has 240 mm flange width and web depth were chosen and subjected to compression loading. Table 2 shows good agreement between experimental results and results of developed FE model.

**Table 2.** Comparison of F.E.M. and experimental results

Specimen	Length(mm)	Experimental Ultimate Load (kN)	F.E.M. Ultimate Load (kN)	$F_{F.E.M.}/F_{Exp.}$
310-5800-A	5800	750.0	770.5	1.0273
240-5800-A	5800	626.0	639.8	1.0220

The results obtained in sections 3.1 and 3.2 verify the accuracy of developed FE models. In the forthcoming section, obtained results of numerical simulations within the framework of section 2 are elaborately presented.

#### 4. Results of Numerical Analyses

In order to draw load-end shortening and load-lateral displacement curves 57 runs have been carried out. All models were generated with end plate. End shortening values have been taken from the loaded end at midpoint of the web and lateral displacement values have been taken from  $z = L/2$  at midpoint of web. Global modes of failures were observed in all specimens and loading conditions. The slope of load-displacement curves changes according to column length, imperfection magnitude and loading eccentricity.

The ultimate loads of end plated columns with  $L/5000$  overall imperfection have been taken as baseline cases for comparison purposes. Figure 7 shows the resulting load versus end shortening and lateral displacement curves, together with the baseline case with  $L/5000$  overall imperfection.

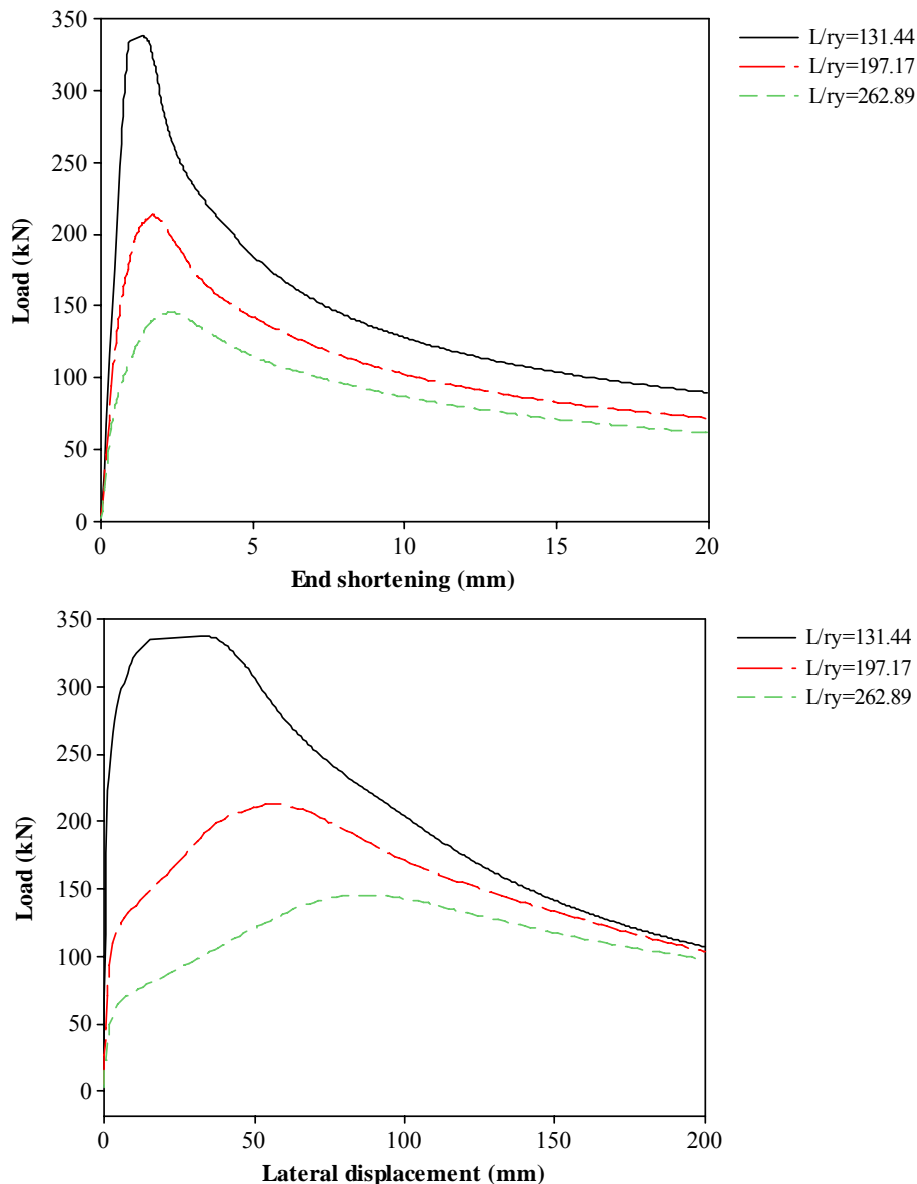


**Figure 7.** Load vs end shortenings and lateral displacements of baseline columns

Figure 7 clearly demonstrate the high degree of sensitivity to slenderness ratio,  $L/r_y$ . The slope of load displacement paths up to limit points decreases with increase of column slenderness ratios. However, slenderness ratio slightly affects end shortening capacity and it is obvious

that lateral displacement capacity up to limit points tends to increase greatly with increase of slenderness ratio. In Figure 8 the load versus displacement curves have been drawn with normalizing ultimate axial loads,  $F_u$ , with respect to the ultimate loads of the columns with  $L/5000$  overall imperfection.

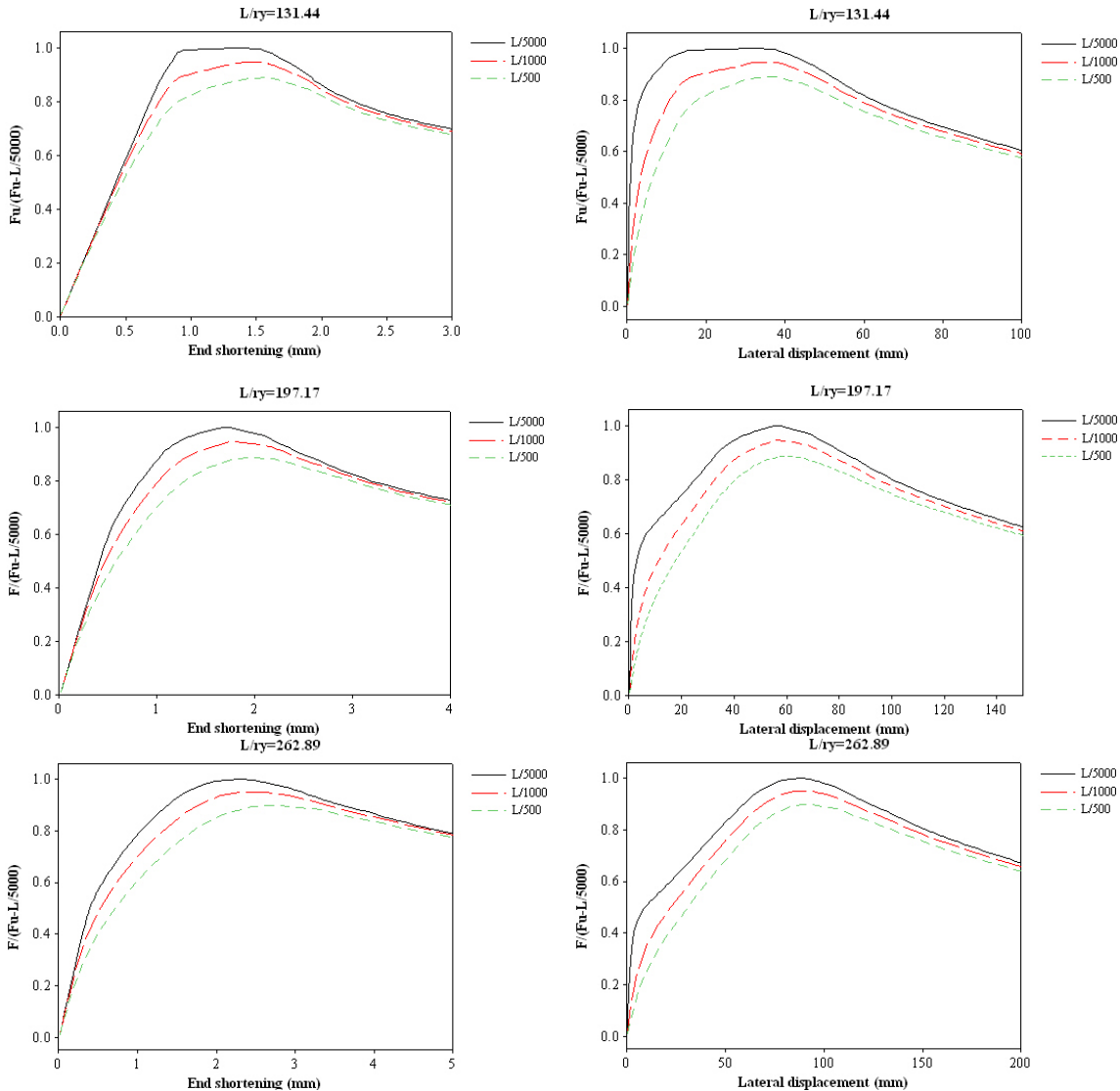


**Figure 8.** Comparison of load vs. displacement curves for different imperfection magnitudes

The load carrying capacity of a corresponding real column depends not only on the imperfection magnitude, but also on the nature of the loading positions, which determines the sensitivity of the column to eccentric loadings. In order to assess the effect of eccentric loadings on the ultimate capacity of columns eccentric end plate point loads were introduced in to the developed FE model. Table 3 provides a concise summary of the results of current phase of work and attempts to quantify their implications.

**Table 3.** Results of eccentric loadings with and without imperfection

Column Length	Eccentricity (mm)		Ultimate (kN)	Load	% Reduction wrt. baseline column		% Differences in reduction
	$e_x$	$e_y$	Imperfection( $\delta$ )		Imperfection( $\delta$ )		
			0	L/1000	0	L/1000	
3.0 m	12.5	0	282.46	266.01	16.36	21.23	4.87
	25.0	0	235.76	225.35	30.19	33.27	3.08
	37.5	0	203.75	195.79	39.67	42.02	2.36
	50.0	0	180.85	174.62	46.45	48.29	1.84
	12.5	25.0	277.00	261.55	17.98	22.55	4.57
	25.0	50.0	226.61	217.35	32.90	35.64	2.74
	37.5	75.0	192.20	185.42	43.09	45.09	2.01
	50.0	100.0	168.14	160.62	50.21	52.44	2.23
4.5 m	12.5	0	190.57	179.48	10.72	15.91	5.19
	25.0	0	167.98	159.86	21.30	25.11	3.81
	37.5	0	151.58	145.46	28.99	31.85	2.86
	50.0	0	139.36	133.46	34.71	37.47	2.76
	12.5	25.0	187.16	176.75	12.32	17.19	4.88
	25.0	50.0	162.31	154.97	23.96	27.40	3.44
	37.5	75.0	144.28	137.76	32.41	35.46	3.05
	50.0	100.0	129.64	125.27	39.26	41.31	2.05
6.0 m	12.5	0	136.74	127.70	6.07	12.28	6.21
	25.0	0	125.52	117.60	13.78	19.22	5.44
	37.5	0	116.84	109.91	19.74	24.50	4.76
	50.0	0	109.72	103.89	24.64	28.64	4.01
	12.5	25.0	135.67	126.83	6.81	12.88	6.07
	25.0	50.0	122.84	115.63	15.63	20.58	4.95
	37.5	75.0	112.68	106.59	22.60	26.78	4.18
	50.0	100.0	104.16	98.98	28.46	32.01	3.55

Drastic results may emerge in structural members when eccentric loadings are integrated with geometrical imperfections. With this intent, along with the eccentric loadings, L/1000 overall geometric imperfections about minor axis were incorporated in to the developed FE model. The results obtained from eccentric loadings with L/1000 geometric imperfections were presented in fifth column of Table 3. The sixth and seventh columns of Table 3 represent the percent reduction in ultimate capacity of corresponding eccentric loadings and eccentric loadings with L/1000 overall imperfection respectively with respect to baseline columns.

For all  $L/r_y$  ratios and loadings global modes of failures were observed as expected. Figure 9 shows deformed shapes of two columns at corresponding failure loads. It can be observed in Figure 9b that  $e_y$  eccentric loading along with  $e_x$  brings about flexural-torsional modes.

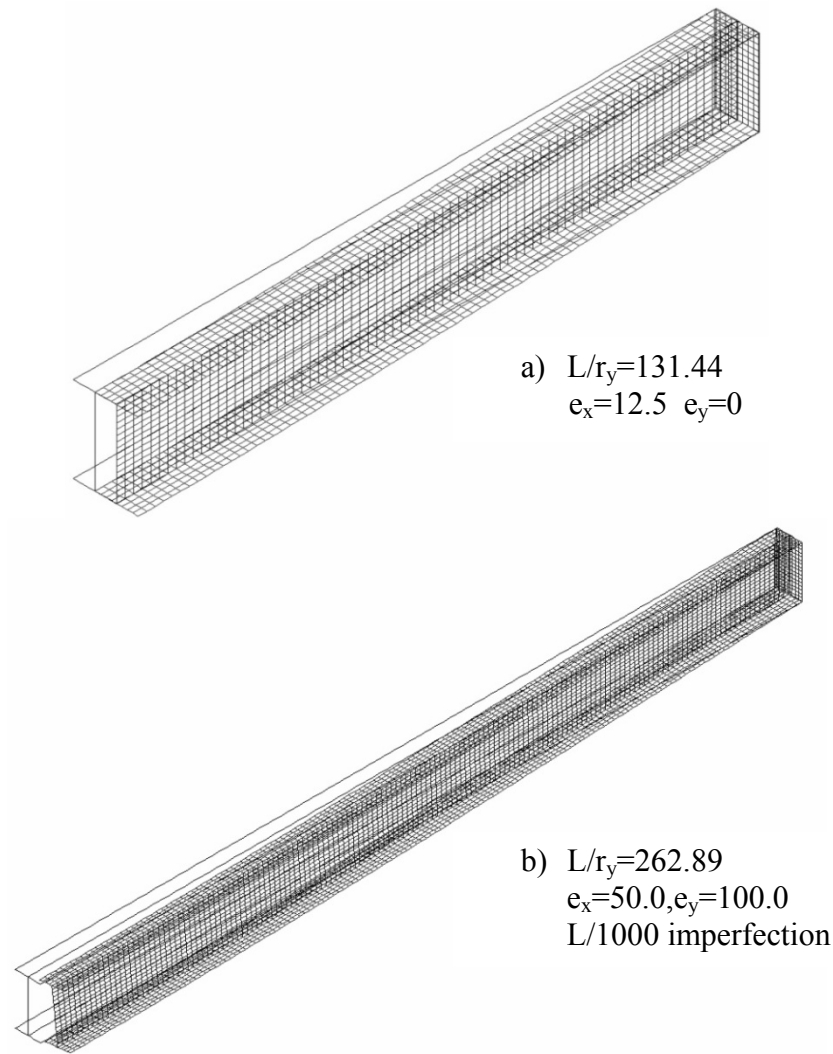


**Figure 9.** Global modes of failure a) flexural b) flexural-torsional

## 5. Discussion of Results

In the present paper the particular concern is with the analysis of the post-buckling behavior under axial loading of IPE 200 column. For this purpose 57 runs were carried out to assess the contributions of imperfection and eccentric loading to reduction of ultimate capacity. The resulting responses were presented in Figure 8 and Table 3. The results presented herein indicate that eccentricity and geometric imperfections can lead to drastic reductions of ultimate strength.

Firstly, analyses results suggests that ultimate loads of IPE 200 cross section range from about 16.36% to nearly 52.44% , 10.72% to 41.32% and 6.07% to 32.01% lower than their baseline cases for 3m, 4.5m and 6m column lengths respectively.

As expected, it can be seen from Table 3 that the ultimate capacity decreases significantly with an increase of the eccentricity and the ultimate loads decreased by 50.21%, 39.26% and 28.46% to be 168.14, 129.64 and 104.16 kN for 3, 4.5 and 6m column lengths respectively, in which case the failure modes become a global one. It is important to highlight that the effect of eccentric loading on the percent drop of ultimate strength decreases as the column length increases.

The results given by solutions for eccentric loadings were compared with the results given by the eccentric loadings with  $L/1000$  overall imperfection. The last column of Table 3 shows additional loss of ultimate capacity by incorporating  $L/1000$  imperfection in to the eccentric loading models. It is of interests to highlight that effect of imperfection on eccentric loading capacity reductions decreases as the eccentricity increases. On the contrary, the contribution of imperfection to capacity loss of eccentric loadings increases with the increase of column length.

## 6. Conclusions

The analysis of the post-buckling behavior of columns is a topic of considerable technical importance in engineering. Presence of geometric imperfections and eccentric loadings lead to significant reduction of post-buckling response of columns. Many studies concerning these effects have been presented in the literature over the last decades. One heading that is not documented in any detail is the post-buckling response of columns subjected to eccentric loadings with geometrical imperfections. In order to investigate these effects the computational study was divided into three phases for different  $L/r_y$  ratios. In the first one, the behavior of I-columns with geometrical imperfections was studied, in the second phase, the effects of eccentric loading on the perfect I-columns investigated and during the last phase, the combination of imperfection and eccentric loading was studied. The nonlinear analyses were carried out via FE method using the commercial code ANSYS.

The work reported in the preceding sections has revealed several main conclusions. It is shown that eccentricity and imperfection causes significant reductions in ultimate capacity of columns. Firstly, the effect of eccentric loading on the percent reduction of ultimate strength decreases as the column length increases. The subsequent phase of the work consists in the introduction of the  $L/1000$  geometrical imperfections in the numerical model. The observed structural responses imply that introducing geometric imperfections in to the eccentric loading models cause reductions in ultimate capacity with different magnitudes according to position of eccentric loading. It is shown that effect of imperfection on eccentric loading capacity reductions decreases as the eccentricity increases. On the contrary, the contribution of imperfection to capacity loss of eccentric loadings increases with the increase of column length.

The present study may bear on a variety of engineering applications and will lead to an improved understanding of the mechanics involved and promisingly build a basis for more realistic and accurate design procedures in the future.

## References

- American Institute of Steel Construction (AISC). (2005). Manual for Structural Steel Buildings: Load and Resistance Factor Design (LRFD), Chicago.
- ANSYS, (2007). User's Manual Release, Canonsburg, Pennsylvania.
- Dauids, A.J., Hancock, G.J. (1986). Compression tests of long welded I-sections columns. J Struct. Engng. ASCE, 112(10), 2281–97.
- European Committee for Standardisation. (2005). EN 1993-1-4: Eurocode-3 Design of steel structures, Part 1-4: General rules—Supplementary rules for stainless steel. Brussels.

- Feng, M., Wang, Y.C. and Davies, J.M. (2004). A numerical imperfection sensitivity study of cold-formed thin-walled tubular steel columns at uniform elevated temperatures. *Thin-Walled Structures*, 42(4), 533-555.
- Gao, L., Sun, H., Jin, F. and Fan, H. (2009). Load carrying capacity of high strength steel box sections I: Stub columns. *Journal of Constructional Steel Research*, 65(4), 918-924.
- Greiner, R. and Kettler, M. (2008). Interaction of bending and axial compression of stainless steel members. *Journal of Constructional Steel Research*, 64(11), 1217-1224.
- Hasham, A.S. and Rasmussen, K.J.R. (2002). Interaction curves for locally buckled I-section beam-columns. *Journal of Constructional Steel Research*, 58(2), 213-241.
- Pan, H., Guo, Y., Liang, S., Pei, S., Liang, W. and Wang, L. (2008). Stability analysis of large diameter thin-walled tube beam columns. *Front. Archit. Civ. Eng.*, 2(2), 123-132.
- Raftoyiannis, I.G. and Ermopoulos, J. C. (2005). Stability of tapered and stepped steel columns with initial imperfections. *Engineering Structures*, 27(8), 1248-1257.
- Rasmussen, K.J.R., Burns, T. (2003). Bezkorovainy P, Bambach MR. Numerical modeling of stainless steel plates in compression. *Journal of Constructional Steel Research*, 59(11),1345-1362.
- Ren, W-X, Zeng, Q-Y. (1997). Interactive buckling behavior and ultimate load of I-section steel columns. *J Struct. Engng. ASCE*, 123(9), 1210–1217.
- Salem, A.H., Aghoury, M.El, Dib, F.F. El and Hanna, M.T. Ultimate capacity of I-slender section columns. (2004). *Journal of Constructional Steel Research*, 60(8), 1193-1211.